# Optomechanically induced transparency in a Laguerre-Gaussian rotational-cavity system and its application to the detection of orbital angular momentum of light fields

Jia-Xin Peng, Zheng Chen, Qi-Zhang Yuan, and Xun-Li Feng*
*Department of Physics, Shanghai Normal University, Shanghai 200234, China*

(Received 24 January 2019; published 15 April 2019)

In this paper, we investigate the optomechanically induced transparency (OMIT) phenomenon in the Laguerre-Gaussian (L-G) rotational-cavity optomechanical system, which can be regarded as an analog of the OMIT in a cavity optomechanical system with a vibrational mirror. We find that the window width of OMIT is dependent on the orbital angular momentum of the L-G light, which can be used to detect the orbital angular momentum of L-G light. We then accordingly propose a scheme to measure the orbital angular momentum of L-G light with OMIT, and its feasibility is justified by numerical simulation.

DOI: 10.1103/PhysRevA.99.043817

## I. INTRODUCTION

Electromagnetically induced transparency (EIT) is a kind of quantum interference effect which occurs in multilevel atoms and manifests itself as a cancellation of absorption in the presence of a strong auxiliary laser field [1]. This effect plays a key role in modern quantum optics experiments and in applications such as quantum memory [2–4], vibrational cooling [5], optical switch [6], and so forth. Very recently, EIT phenomenon for the atomic medium driven by a Laguerre-Gaussian (L-G) beam mode was investigated in Refs. [7,8]. The EIT analog occurring in an optomechanical system is called optomechanically induced transparency (OMIT), which was first predicted theoretically [9–11] and observed experimentally [12–14]. Subsequently, its applications in several fields were presented in vibrating cavity optomechanical systems, such as controlling the probe field in a single-photon Fock-state [15], controlling the speed of light [13], measuring the electrical charge [16], the mass of mechanical resonator [17], and the environmental temperature [18].

In 2007, Bhattacharya and Meystre proposed an L-G rotational-cavity optomechanical system [19] which is composed of two spiral phase elements acting as cavity mirrors, a fixed mirror, and a rotating one about the cavity axis. In such an optomechanical system, the cavity mode is L-G light which carries orbital angular momentum and can exchange orbital angular momentum with spiral phase elements. Now, more and more attention has been paid to such systems and interesting results about cooling of rotational mirrors [20], two entanglements of an L-G light with a rotational mirror [21], and that between a vibrational and a rotational mode of the mirror [22] were obtained. Recently, based on the theory of ray transfer matrix, Eggleston *et al.* investigated the stability of a cavity consisting of two spiral phase plates in the case of incident rays far from the center of the cavity [23]. However, to the best of our knowledge, the study about the OMIT in this system has not been reported until now.

On the other hand, measuring the orbital angular momentum of L-G light plays a significant role in optical communications [24–26], encoding information [27], and detection of rotating objects [28], etc., and various measurement schemes have been proposed to do so. In general, measuring the orbital angular momentum of L-G light requires knowing the information of the phase distribution around a singularity, but it is generally impossible to directly measure the phase of far-field in the visible light. A commonly used technique is to interfere a flat wave front with the spiral wave front in an interferometer and then to determine the orbital angular momentum by counting the number of spiral fringes [29]. Besides, phase-stepping techniques [30] and cascading additional Mach-Zehnder interferometers [31] were developed to measure orbital angular momentum of a single photon. Very recently, Zheng and Wang utilized a ring grating to measure the L-G light of different orders and the highest measurable topological charge can reach $l = |25|$ [32].

In this paper, we investigate the OMIT in the L-G rotational-cavity optomechanical system, and find that the window width of OMIT depends on the orbital angular momentum of L-G light. We then accordingly propose a scheme to measure the orbital angular momentum of L-G light with OMIT. Our scheme can efficiently measure a wide range of orbital angular momentum of the L-G light with the topological charge range from zero up to 42. Besides, this scheme works better for the case of the high-order topological charge.

The paper is organized as follows. In Sec. II, we introduce the model for the optomechanical system of OMIT in detail. In Sec. III, the steady state of the system and the quadrature of the output field are given. In Sec. IV, the OMIT is studied in the homodyne spectrum of the output field. In Sec. V, we propose a scheme to detect orbital angular momentum of L-G light. The last section concludes this paper.

*xlfeng@shnu.edu.cn

 

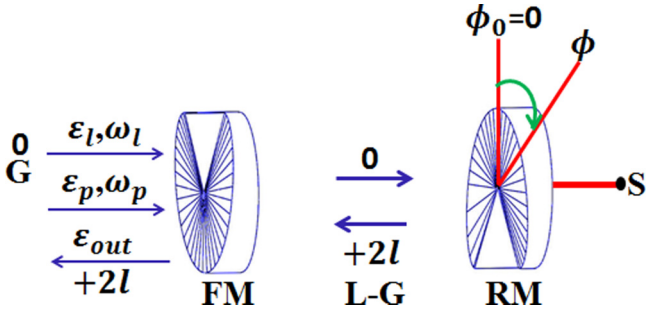


FIG. 1. Schematic diagram of the system consists of an optomechanical cavity with a rigidly fixed mirror FM and a rotational one RM, the cavity mode is the L-G mode and is driven by a strong pumping field $\varepsilon_l$. A weak field $\varepsilon_p$ acts as probe to detect response of the system. The output field is represented by $\varepsilon_{\text{out}}$. The equilibrium position of the rotational mirror is $\phi_0$, and the angular displacement is indicated by angle $\phi$ under the action of the torsion. The charge on the beams at various points has been indicated.

## II. MODEL AND HAMILTONIAN

As shown in Fig. 1, the model of an optomechanical cavity we consider here is similar to that in Ref. [19], where both mirrors are the spiral phase elements with one rigidly fixed and the other, mounted on a support $S$, being able to rotate about the cavity axis. The fixed mirror is partially transmitting and does not change the topological charge of any beams passing through it, while the reflection on it gives a mode with charge 0. In addition, the rotational mirror is perfectly reflective and it can add a topological charge $2l$ to its reflected light beam. A strong pumping field (Gaussian beam) $\varepsilon_l$ with zero topological charge is injected to the optomechanical system and drives the L-G cavity mode of the frequency $\omega_c$. The other field $\varepsilon_p$, the weak probe, is used to detect the response of the system. We assume that the frequencies of the two light fields are $\omega_l$ and $\omega_p$, respectively. The Hamiltonian of this system takes the form

$$H_1 = \hbar\omega_c a^\dagger a + \frac{L_z^2}{2I} + \frac{1}{2}I\omega_\phi^2\phi^2 - \hbar g_\phi a^\dagger a\phi + i\hbar[(\varepsilon_l e^{-i\omega_l t} + \varepsilon_p e^{-i\omega_p t})a^\dagger - \text{H.c.}], \quad (1)$$

where the first term represents the free Hamiltonian of the L-G cavity mode with $a$ ($a^\dagger$) being the annihilation (creation) operator; the next two terms give the free Hamiltonian of the rotational mirror with $\omega_\phi$ being the angular rotation frequency, $L_z$ the angular momentum, $\phi$ the angular displacement, and $I = MR^2/2$ the moment of inertia of the rotation mirror about the cavity axis; the fourth term represents the optorotational coupling between the L-G cavity mode and the rotational mirror with the coupling strength $g_\phi = cl/L$; and the last term stands for the driving to the cavity mode by the strong pumping field, the weak probe field with amplitudes $\varepsilon_l = \sqrt{2\kappa P_l/\hbar\omega_c}$, and $\varepsilon_p = \sqrt{2\kappa P_p/\hbar\omega_p}$, respectively.

In the rotating frame with respect to the frequency of the pumping field $\omega_l$, the Hamiltonian of Eq. (1) is transformed to

$$H_2 = \hbar\Delta_c a^\dagger a + \frac{L_z^2}{2I} + \frac{1}{2}I\omega_\phi^2\phi^2 - \hbar g_\phi a^\dagger a\phi + i\hbar[(\varepsilon_l + \varepsilon_p e^{-i\delta t})a^\dagger - \text{H.c.}], \quad (2)$$

where $\Delta_c = \omega_c - \omega_l$ is the detuning of the pumping field from the cavity mode and $\delta = \omega_p - \omega_l$ the detuning of the pumping field from the probe field.

## III. MEAN VALUE EQUATIONS AND QUADRATURES OF THE OUTPUT FIELD

In this section, let us first examine the time evolution of the optomechanical system. From the Hamiltonian Eq. (2), one can get the Heisenberg equations of the operators of the system and then, adding the damping terms to them, we can finally obtain the mean-value equations of the system,

$$\begin{aligned}\left\langle\frac{d\phi}{dt}\right\rangle &= \frac{\langle L_z\rangle}{I},\\ \left\langle\frac{dL_z}{dt}\right\rangle &= -I\omega_\phi^2\langle\phi\rangle + \hbar g_\phi\langle a^\dagger\rangle\langle a\rangle - \gamma_\phi\langle L_z\rangle,\\ \left\langle\frac{da}{dt}\right\rangle &= -[\kappa + i(\Delta_c - g_\phi\phi)]\langle a\rangle + \varepsilon_l + \varepsilon_p e^{-i\delta t},\end{aligned} \quad (3)$$

where $\gamma_\phi$ is introduced as the intrinsic damping rate of the rotational mirror, $\kappa$ is the decay rate of the L-G cavity, and the coarse grain approximation $\langle AB\rangle = \langle A\rangle\langle B\rangle$ [10] is used. Therefore, the steady-state values of the dynamical variables are

$$\phi_s = \frac{\hbar g_\phi|a_s|^2}{I\omega_\phi^2}, \quad L_{z,s} = 0,$$
$$a_s = \frac{\varepsilon_l}{\kappa + i\Delta}, \quad |a_s|^2 = \frac{|\varepsilon_l|^2}{\kappa^2 + \Delta^2}, \quad (4)$$

where $\Delta = \Delta_c - g_\phi\phi_s$, effective detuning between the cavity mode and the driving field.

Now, we consider the quantum fluctuation effect on the system. The operator around their steady-state values can be linearized in the usual way as $a = a_s + \delta a$; here $\delta a$ is quantum fluctuation, similarly for the other operators. Usually the mean value of the physical quantity is much larger than its fluctuation, hence neglecting the nonlinear terms (e.g., $\delta a\delta a^\dagger$) is reasonable and we can obtain the linearized quantum Langevin equations [33]:

$$\begin{aligned}\dot{\delta\phi} &= \frac{\delta L_z}{I},\\ \dot{\delta L_z} &= -I\omega_\phi^2\delta\phi + \hbar g_\phi(a_s^*\delta a + a_s\delta a^\dagger) - \gamma_\phi\delta L_z,\\ \dot{\delta a} &= -(\kappa + i\Delta_c)\delta a + ig_\phi(\delta a\phi_s + \delta\phi a_s) + \varepsilon_p e^{-i\delta t}.\end{aligned} \quad (5)$$

For the sake of simplicity, by applying the following ansatz [10]:

$$\begin{aligned}\delta\phi &= \delta\phi_+\varepsilon_p e^{-i\delta t} + \delta\phi_-\varepsilon_p^* e^{i\delta t},\\ \delta L_z &= \delta L_{z+}\varepsilon_p e^{-i\delta t} + \delta L_{z-}\varepsilon_p^* e^{i\delta t},\\ \delta a &= \delta a_+\varepsilon_p e^{-i\delta t} + \delta a_-\varepsilon_p^* e^{i\delta t},\end{aligned} \quad (6)$$

Eqs. (5) can be transformed into the following form:

$$\begin{aligned}\delta L_{z+} + iI\delta\delta\phi_+ &= 0,\\ \delta L_{z-} - iI\delta\delta\phi_- &= 0,\\ \delta L_{z+}(\gamma_\phi - i\delta) + I\omega_\phi^2\delta\phi_+ &= \hbar g_\phi(a_s^*\delta a_+ + a_s\delta a_-^\dagger),\end{aligned}$$

$$\delta L_{z-}(\gamma_\phi + i\delta) + I\omega_\phi^2 \delta\phi_- = \hbar g_\phi (a_s^* \delta a_- + a_s \delta a_+^\dagger),$$
$$(\omega_\phi^2 - \delta^2 - i\gamma_\phi)\delta\phi_+ = \frac{\hbar g_\phi}{I}(a_s^* \delta a_+ + a_s \delta a_-^\dagger), \quad (7)$$
$$(\omega_\phi^2 - \delta^2 + i\gamma_\phi)\delta\phi_- = \frac{\hbar g_\phi}{I}(a_s^* \delta a_- + a_s \delta a_+^\dagger).$$

We can then obtain the solution of $\delta a_+$,

$$\delta a_+ = \frac{\left[(\omega_\phi^2 - \delta^2 - i\gamma_\phi)G_+ I + i\hbar g_\phi^2 |a_s|^2\right]}{(\omega_\phi^2 - \delta^2 + i\gamma_\phi)G_+ G_- I - i\hbar g_\phi^2 |a_s|^2 (G_+ - G_-)}, \quad (8)$$

where $G_+ = \kappa - i\Delta_c + ig_\phi \phi_s - i\delta$ and $G_- = \kappa + i\Delta_c - ig_\phi \phi_s - i\delta$, and $|a_s|^2$ is the mean photon number of the cavity field.

Using standard input-output relation [31], the output field is given by

$$\varepsilon_{out} = \varepsilon_{in} - 2\kappa a$$
$$= \varepsilon_l + \varepsilon_p e^{-i\delta t} - 2\kappa(a_s + \delta a_+ \varepsilon_p e^{-i\delta t} + \delta a_- \varepsilon_p^* e^{i\delta t}), \quad (9)$$

and the transmission of the probe field is given by [9]

$$t_p = \frac{\varepsilon_p - 2\kappa \delta a_+ \varepsilon_p}{\varepsilon_p}$$
$$= 1 - 2\kappa \delta a_+, \quad (10)$$

which can be measured by homodyne detecting technique [30]. In practice, OMIT phenomenon is described by quadrature $\varepsilon_T$ of the optical components in the output field,

$$\varepsilon_T = 2\kappa \delta a_+$$
$$= 2\kappa \frac{\left[(\omega_\phi^2 - \delta^2 - i\gamma_\phi)G_+ I + i\hbar g_\phi^2 |a_s|^2\right]}{(\omega_\phi^2 - \delta^2 + i\gamma_\phi)G_+ G_- I - i\hbar g_\phi^2 |a_s|^2 (G_+ - G_-)}$$
$$= \mu_p + i\nu_p, \quad (11)$$

where $\mu_p$ and $\nu_p$ represent the absorptive and dispersive coefficient of the optomechanical system, respectively [10].

In what follows, we will carry out numerical simulations to show the absorptive and dispersive properties in such a system; our results will indicate the existence of the OMIT.

## IV. OMIT IN THE HOMODYNE SPECTRUM OF THE OUTPUT FIELD

In this section, we will examine the absorptive and dispersive properties of the output field with the relation of the power of the pumping field, the mass of the rotational mirror, and orbital angular momentum of the L-G cavity mode, respectively.

Figures 2(a) and 2(b) show that the absorptive and dispersive coefficient as a function of the normalized optical detuning for the different power of pumping field. Here and in what follows, the parameters are chosen [19,21,22]: the cavity length is $L = 5$ mm, the cavity decay rate $\kappa = 2\pi \times 10$ MHz, the wavelength of pumping field $\lambda = 810$ nm, and the angular frequency, radius, and decay rate for the rotation mirror are $\omega_\phi = 2\pi \times 46$ MHz, $R = 100$ $\mu$m, and $\gamma_\phi = 2\pi \times 140$ Hz, respectively.

From Fig. 2(a), we can see that when the power of pumping field is equal to zero, the absorption curve of quadrature of the outfield is a standard Lorentzian-shaped line. However, when the power of pumping field is not equal to zero, the absorptive curve sharply drops, forming a clear transparent window when the normalized optical detuning approaches zero, and this is typical EIT-like line shape. The result reflects the fact that the pumping field leads to destructive interference between the probe field and the scattering cavity field. In addition, the window width of OMIT is enhanced with the increase of the power of the pumping field. Figure 2(b) shows that when the pumping field exists, the probe field will undergo a sharp dispersion change. Apparently, the OMIT phenomenon occurring in the system with rotational cavity mirror is very similar to that in the system with vibrational cavity mirror [9,10].

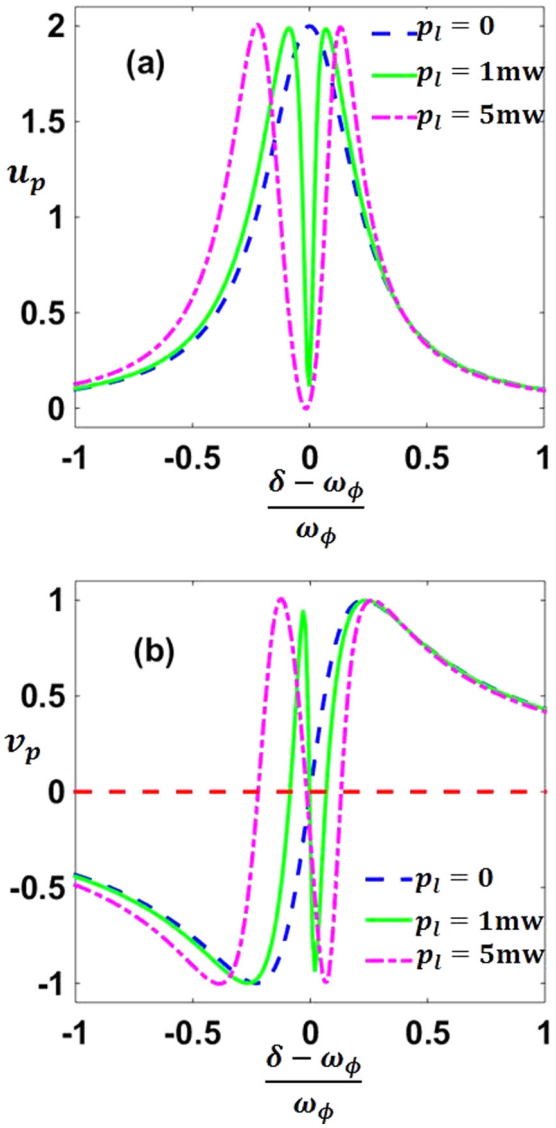


FIG. 2. The absorption curves (a) and dispersion curves (b) as functions of the normalized optical detuning when the orbital angular momentum of L-G light is 35, mass of the rotational mirror is $m = 2$ mg, and the powers of the pumping field are $p_l = 0$, $p_l = 1$ mw, and $p_l = 5$ mw, respectively.

Presented in Fig. 3 is the absorptive coefficient depending on the normalized optical detuning under the different mass

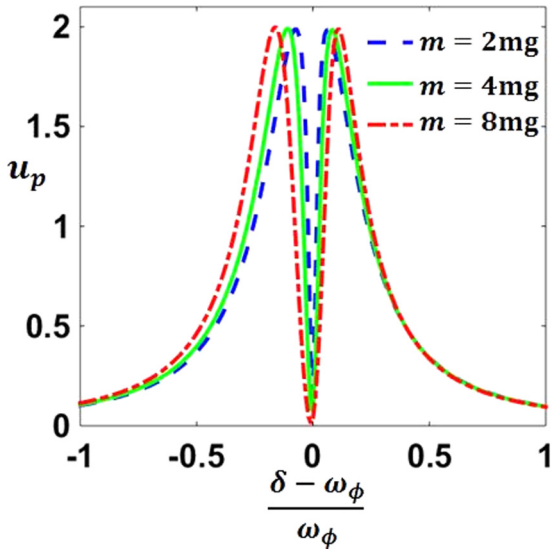


FIG. 3. The absorption curve as a function of the normalized optical detuning with the orbital angular momentum of L-G light being 35 and the mass of the rotational mirror being $m = 2$ mg, $m = 4$ mg, and $m = 8$ mg, respectively.

of the rotational mirror. It shows that the window width of the OMIT becomes wider as the mass of the rotational mirror decreases.

Figure 4 represents the absorptive curve as a function of the normalized optical detuning with different orbital angular momentum of the L-G cavity mode, and it shows that the window width of OMIT becomes wider as the orbital angular momentum increases. The feature that the window width of OMIT depends on the orbital angular momentum of the L-G cavity mode reminds us that it is possible to detect the orbital angular momentum by using the window width of the OMIT. In fact, for our convenience we will adopt the left extreme point in each curve as a measure of the orbital angular momentum. To this end, in the following section we

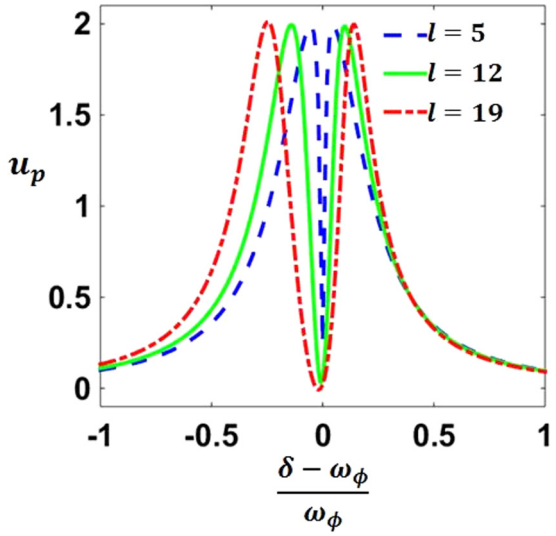


FIG. 4. The absorption curve as a function of the normalized optical detuning in the case of $m = 1$ mg, $p_l = 10$ mw, and different orbital angular momentum: $l = 5$, $l = 12$, and $l = 19$, respectively.

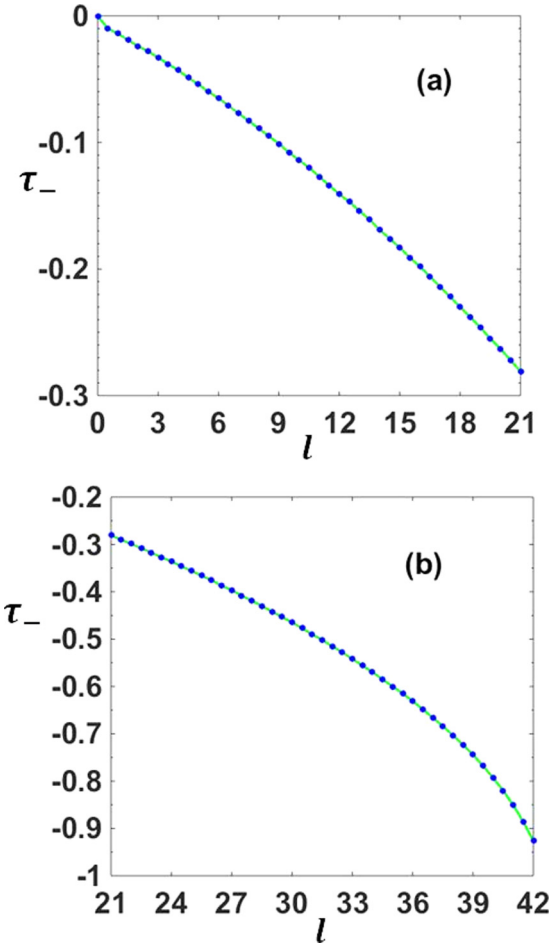


FIG. 5. (a) ($l = 0 \sim 21$) and (b) ($l = 21 \sim 42$) plot the dependence of $\tau_-$ on the orbital angular momentum of L-G light where the topological charge $l$ changes in a unit of half integer.

will investigate in detail the relation between the position of left extreme point and orbital angular momentum.

## V. MEASUREMENT OF THE ORBITAL ANGULAR MOMENTUM OF L-G LIGHT

In this section, we will apply OMIT phenomenon to detect the orbital angular momentum of L-G light. As shown in Fig. 4, each absorption curve of the output field has two extreme points which are determined by the conditions

$$\frac{d\mu_p}{d\tau}\Big|_{\tau=\tau_\pm} = 0, \quad \frac{d^2\mu_p}{d\tau^2}\Big|_{\tau=\tau_\pm} < 0, \tag{12}$$

where $\tau = \delta - \omega_\phi$. $\tau_-$ corresponds to the position of the left extreme point and $\tau_+$ that of the right one. Figure 4 also shows that the absorption curve of the output field is asymmetric about $\tau = 0$ and $\tau_-$ changes more obviously than $\tau_+$ with the change of orbital angular momentum, which implies that the position of the left extreme point is more sensitive to the change of the orbital angular momentum. So, in the following, we will adopt $\tau_-$ as the measure of the orbital angular momentum.

Figures 5(a) ($l = 0 \sim 21$) and 5(b) ($l = 21 \sim 42$) plot the dependence of $\tau_-$ on the orbital angular momentum of L-G

light where the topological charge $l$ changes in a unit of half integer with the $m = 1$ mg and the $p_l = 10$ mw. Both curves show that the topological charge $l$ can be read clearly by $\tau_-$. Besides, in comparison with other schemes [30–32], our scheme can detect a wider range of orbital angular momentum, and the highest measurable orbital angular momentum is even as high as 42. Furthermore, we notice that for $l = 0 \sim 21$, the change of $\tau_-$ is from 0 to $-0.281$ in Fig. 5(a), while for $l = 21 \sim 42$, the change of $\tau_-$ is from $-0.281$ to $-0.926$ in Fig. 5(b), which indicates that the high-order topological charge is easier to distinguish. Particularity, for the range of topological charge from 30 to 42, this effect is more obvious. Therefore, our scheme works better for the high-order topological charge $l = 30 \sim 42$.

Finally, we should point out that our scheme cannot distinguish the sign of orbital angular momentum, this is a shortage of our scheme, which also exists in some other schemes [31,34,35].

## VI. CONCLUSION

In summary, we have investigated the absorptive and dispersive properties of the output field of L-G rotational-cavity optomechanical system and demonstrated the existence of the OMIT phenomenon, which is very similar to that in the system with vibrational cavity mirror. Moreover, we have found that the window width of OMIT depends on the orbital angular momentum of L-G light and thus can be used to detect the orbital angular momentum of L-G light by resorting to window information of OMIT. We then accordingly propose a scheme to measure the orbital angular momentum of L-G light, which can efficiently detect a wide range of orbital angular momentum of the L-G light with the topological charge range from zero up to 42. In addition, our scheme works better for L-G light with the high-order topological charge. We believe that our scheme provides a new path for the realization of orbital angular momentum detectors.

Finally, as a remark, we mention that more analysis is required for deciding the stability of the cavity we have proposed since stability criteria have been investigated in such cavities only for rays far off center [23], in particular the Gaussian ($l = 0$) mode will diffract considerably from the sharp edge near the plate center leading to diffractive loss. We will further investigate such a question elsewhere.

## ACKNOWLEDGMENTS

This work is supported National Natural Science Foundation of China under Grants No. 61475168, No. 11674231, No. 11074079, and No. 11804225 and Ministry of Science and Technology of the People's Republic of China (No. 2018YFA0404803). X.L.F. is sponsored by Shanghai Gaofeng & Gaoyuan Project for University Academic Program Development.

[1] M. Aspelmeyer, T. J. Kippenberg, and F. Marquardt, Rev. Mod. Phys. **86**, 1391 (2014).
[2] A. I. Lvovsky, B. C. Sanders, and W. Tittel, Nat. Photon. **3**, 706 (2009).
[3] I. Novikova, R. Walsworth, and Y. Xiao, Laser Photon. Rev. **6**, 333 (2012).
[4] V. M. Acosta, K. Jensen, C. Santori, D. Budker, and R. G. Beausoleil, Phys. Rev. Lett. **110**, 213605 (2013).
[5] J. Q. Zhang, S. Zhang, J. H. Zou, L. Chen, W. Yang, Y. Li, and M. Feng, Opt. Express **21**, 29695 (2013).
[6] J. Q. Shen and S. He, Phys. Rev. A **74**, 063831 (2006).
[7] J. Anupriya, N. Ram, and M. Pattabiraman, Phys. Rev. A **81**, 043804 (2010).
[8] T. G. Akin, S. P. Krzyzewski, A. M. Marino, and E. R. I. Abraham, Opt. Commun. **339**, 209 (2015).
[9] S. Weis, R. Riviere, S. Deleglise, E. Gavartin, O. Arcizet, A. Schliesser, and T. J. Kippenberg, Science **330**, 1520 (2010).
[10] G. S. Agarwal and S. Huang, Phys. Rev. A **81**, 041803(R) (2010).
[11] H. Xiong, L. G. Si, A. S. Zheng, X. Yang, and Y. Wu, Phys. Rev. A **86**, 013815 (2012).
[12] Q. Lin, J. Rosenberg, D. Chang, R. Camacho, M. Eichenfield, K. J. Vahala, and O. Painter, Nat. Photon. **4**, 236 (2010).
[13] A. H. Safavi-Naeini, T. P. M. Alegre, J. Chan, M. Eichenfield, M. Winger, Q. Lin, J. T. Hill, D. Chang, and O. Painter, Nature (London) **472**, 69 (2011).
[14] J. D. Teufel, D. Li, M. S. Allman, K. Cicak, A. J. Sirois, J. D. Whittaker, and R. W. Simmonds, Nature (London) **471**, 204 (2011).
[15] G. S. Agarwal and S. Huang, Phys. Rev. A **85**, 021801(R) (2012).
[16] J. Q. Zhang, Y. Li, M. Feng, and Y. Xu, Phys. Rev. A **86**, 053806 (2012).
[17] Q. Wang, W. J. Li, P. C. Ma, and Z. He, Int. J. Theor. Phys. **56**, 2212 (2017).
[18] Q. Wang, J. Q. Zhang, P. C. Ma, C. M. Yao, and M. Feng, Phys. Rev. A **91**, 063827 (2015).
[19] M. Bhattacharya and P. Meystre, Phys. Rev. Lett. **99**, 153603 (2007).
[20] Y. M. Liu, C. H. Bai, D. Y. Wang, T. Wang, M. H. Zheng, H. F. Wang, A. D. Zhu, and S. Zhang, Opt. Express **26**, 6143 (2018).
[21] M. Bhattacharya, P. L. Giscard, and P. Meystre, Phys. Rev. A **77**, 013827 (2008).
[22] M. Bhattacharya, P. L. Giscard, and P. Meystre, Phys. Rev. A **77**, 030303(R) (2008).
[23] M. Eggleston, T. Godat, E. Munro, M. A. Alonso, H. Shi, and M. Bhattacharya, J. Opt. Soc. Am. A **30**, 2526 (2013).
[24] J. Wang, J. Y. Yang, Irfan M. Fazal, N. Ahmed, Y. Yan, H. Huang, Y. X. Ren, Y. Yue, S. Dolinar, M. Tur, and Alan E. Willner, Nat. Photon. **6**, 488 (2012).
[25] Y. Yan, Y. Yue, H. Huang, Y. X. Ren, N. Ahmed, M. Tur, S. Dolinar, and A. Willner, Opt. Lett. **38**, 3930 (2013).
[26] Bozinovic, Y. Yue, Y. X. Ren, M. Tur, P. Kristensen, H. Huang, and A. E. Willner, Science **340**, 14545 (2013).
[27] G. Gibson, J. Courtial, M. J. Padgett, M. Vasnetsov, V. Pas'ko, S. M. Barnett, and S. F. Arnold, Opt. Express **12**, 5448 (2004).
[28] M. P. Lavery, F. C. Speirits, S. M. Barnett, and M. J. Padgett, Science **341**, 537 (2013).

[29] M. Harris, C. A. Hill, and J. M. Vaughan, Opt. Commun. **106**, 161 (1994).
[30] J. Leach, J. Courtial, K. Skeldon, S. M. Barnett, S. Franke-Arnold, and M. J. Padgett, Phys. Rev. Lett. **92**, 013601 (2004).
[31] J. Leach, M. J. Padgett, S. M. Barnett, S. Franke-Arnold, and J. Courtial, Phys. Rev. Lett. **88**, 257901 (2002).
[32] S. Zheng and J. Wang, Sci. Rep. **7**, 40781 (2014).
[33] D. F. Walls and G. J. Milburn, *Quantum Optics* (Springer-Verlag, Berlin, 1994).
[34] C. S. Guo, L. L. Lu, and H. T. Wang, Opt. Lett. **34**, 3686 (2009).
[35] C. S. Guo, S. J. Yue, and G. X Wei, Appl. Phys. Lett. **94**, 231104 (2009).